Higgs effects in top quark pair production[†]

R. HARLANDER[a], M. JEŻABEK[a,b] AND J.H. KÜHN[a,c]

[a] *Institut für Theoretische Teilchenphysik, D–76128 Karlsruhe, Germany*
[b] *Institute of Nuclear Physics, Kawiory 26a, PL–30055 Cracow, Poland*
[c] *Stanford Linear Accelerator Center, Stanford, CA 94309*

Abstract

Top quark production in $p\bar{p}$ and e^+e^- collisions is enhanced by the exchange of a Higgs boson. The enhancement factors are calculated in the threshold region using the Greens function method.

The recent discovery of the top quark [1, 2] and its large mass following from both direct [1, 2] and indirect [3] observations necessitate evaluation of Higgs effects for top quark pair production in the threshold region[‡]. It has been observed long ago [4, 5, 6] that these effects can be important for heavy top quarks due to the attractive Yukawa force in $t\bar{t}$–systems. Although this force is weaker than chromostatic interactions its quantitative description will be necessary in future precise studies of the threshold top pair production at both e^+e^- and $p\bar{p}$ colliders. In this article enhancement factors are evaluated for both singlet and octet color configuration of the $t\bar{t}$–system. The former is relevant for e^+e^- annihilation and the latter for $q\bar{q}$ annihilation which dominates at TEVATRON energies. In both cases the effects of Higgs exchange enhance the production cross sections. The perturbative potential depends on the color configuration of $t\bar{t}$. It is proportional to the color factor C_R. For the singlet configuration $C_R = C_1 = -4/3$, for octet $C_R = C_8 = +1/6$. Thus the chromostatic interactions are attractive for singlet and repulsive for octet configurations[§]. The long distance part of the chromostatic potential, which is presumably related to some composite scalar exchange, may depend in a different way on the color configuration of $t\bar{t}$. However, we have checked that the short lifetime of top quarks cuts off contributions corresponding to small momentum transfers.

The threshold behavior of $t\bar{t}$–production is determined by the s– and p–wave Greens functions $G(\mathbf{p}, E)$ and $F(\mathbf{p}, E)$ satisfying the following Lippmann–Schwinger equations:

$$G(\mathbf{p}, E) = G_0(\mathbf{p}, E) + G_0(\mathbf{p}, E) \int \frac{d^3k}{(2\pi)^3} V(\mathbf{p} - \mathbf{k}) G(\mathbf{k}, E) \tag{1}$$

$$F(\mathbf{p}, E) = G_0(\mathbf{p}, E) + G_0(\mathbf{p}, E) \int \frac{d^3k}{(2\pi)^3} \frac{\mathbf{p} \cdot \mathbf{k}}{\mathbf{p}^2} V(\mathbf{p} - \mathbf{k}) F(\mathbf{k}, E) \ , \tag{2}$$

where

$$G_0(\mathbf{p}, E) = \frac{1}{E - \frac{\mathbf{p}^2}{m_t} + i\Gamma_t} \tag{3}$$

and $E = \sqrt{s} - 2m_t$. Γ_t is the width of the top quark taken to be constant.

In [7, 8] these equations were solved numerically for a static potential

$$V_{\text{QCD}}(\mathbf{p}) = C_R \frac{\alpha_{eff}(\mathbf{p})}{\mathbf{p}^2} \ , \tag{4}$$

[‡] The top mass measured by the CDF Collaboration is $m_t = 176 \pm 8(\text{stat.}) \pm 10(\text{sys.})$ GeV and the value obtained by the DØ Collaboration is equal to $m_t = 199^{+19}_{-21}(\text{stat.}) \pm 22(\text{sys.})$ GeV. Indirect determination [3] gives $m_t = 178 \pm 11^{+18}_{-19}$ GeV.

[§] The relation $C_1 + 8C_8 = 0$ follows from the tracelessness of the Gell–Mann matrices: $\text{Tr} \sum_{a=1}^{8} \lambda_a^{(1)} \lambda_a^{(2)} = 0$. The latter equation means that the sum of the color factors for single gluon exchange in the $t\bar{t}$–system vanishes after averaging over all color configurations of $t\bar{t}$. Thus the sum of the color factors for one singlet and eight octet states is equal to zero.

assuming instantaneous gluon exchange between the two quarks. C_R is an $SU(3)$–group theory factor depending on the color state of the $t\bar{t}$–system. The function α_{eff} is described in [9]. Its form follows from the assumption that the QCD–potential is described by a phenomenological Richardson ansatz for small momentum transfers and the perturbative 2–loop formula for intermediate and large ones.

To take Higgs effects into account we follow [10] using the Yukawa potential approach combined with perturbative results. This means that we insert the effective potential

$$V_{\text{eff}} = V_{\text{QCD}} + V_{\text{Yuk}} \tag{5}$$

into eqs.(1) and (2), with V_{QCD} from (4) and

$$V_{\text{Yuk}}(\mathbf{p}) = -\frac{4\pi\kappa}{m_H^2 + \mathbf{p}^2} \quad, \tag{6}$$

$$\kappa = \sqrt{2}G_F m_t^2/4\pi \quad. \tag{7}$$

The outcome $G(\mathbf{p}, E)$ for the numerical evaluation of (1) then has to be multiplied by the energy independent factor

$$1 + \frac{\kappa}{\pi}\widehat{f}_V(m_H^2/m_t^2) \quad, \tag{8}$$

with

$$\widehat{f}_V(m_H^2/m_t^2) = f_{\text{thr}}(m_H^2/m_t^2) - \pi\frac{m_t}{m_H} \quad. \tag{9}$$

f_{thr} is the perturbatively evaluated threshold correction function and can be written as [11]

$$f_{\text{thr}}(r) = -\frac{1}{12}\left[-12 + 4r + (-12 + 9r - 2r^2)\ln r + \frac{2}{r}(-6 + 5r - 2r^2)l_4(r)\right] \,, \tag{10}$$

with

$$l_4(r) = \begin{cases} \sqrt{r(4-r)}\arccos(\sqrt{r}/2) & \text{if} \quad r \le 4 \,, \\ -\sqrt{r(r-4)}\frac{1}{2}\ln\frac{1+\sqrt{1-4/r}}{1-\sqrt{1-4/r}} & \text{if} \quad r > 4 \,. \end{cases} \tag{11}$$

For the singlet case the effect on the total cross section can therefore be summarized by the following replacement of the lowest order phase space factor $\beta = \sqrt{1 - 4m_t^2/s}$:

$$\beta \rightarrow \left(1 - \frac{8\alpha_s}{3\pi}\right)^2 B(E) \quad, \tag{12}$$

with

$$B(E) = \left(1 + \frac{\kappa}{\pi}\widehat{f}_V(m_H^2/m_t^2)\right)^2 \frac{2\Gamma_t}{m_t^2\pi}\int_0^\infty dp\,p^2|G(\mathbf{p}, E)|^2 \quad. \tag{13}$$

3

Expecting the main effect to come from the modification $V_{\mathrm{QCD}} \to V_{\mathrm{QCD}} + V_{\mathrm{Yuk}}$ and realizing the attractive character of V_{Yuk}, the production cross section should be enhanced with the global factor (8) giving damping corrections to this enhancement.

Considering first e^+e^- annihilation, the $t\bar{t}$–system is produced in a color singlet state and the group theory factor is given by $C_R = -4/3$. Therefore, V_{QCD} is attractive enabling resonance $t\bar{t}$–production below threshold. The width of the top quark largely smears these resonances such that in fig.1(a) only the $1s$–peak remains visible. The solid line corresponds to the case without Higgs exchange. The dashed one shows the behavior for $M_H = 100$ GeV, the dotted one for $M_H = 60$ GeV. In fig.2(a) the ratio of the cross section for different values of the Higgs mass to the one without Higgs is plotted in an energy range from -10 to $+30$ GeV around threshold. It strongly varies in the region around the $1s$–resonance for small values of M_H: Reaching a maximum of about 24%, it rapidly goes down to 10% until the cross section passes into the continuum like region built up by the overlapping higher resonances. The maximum is less pronounced for a larger Higgs mass, flattening down to about 3% for $M_H = 300$ GeV. For $E > 0$ the energy dependence becomes weaker with the curve getting nearly constant for $M_H = 300$ GeV.

In case of polarized electron and/or positron beams the angular distribution and the components of the polarization vector are governed by the function

$$\Phi(E) = \frac{(1 - 4\alpha_s/3\pi)}{(1 - 8\alpha_s/3\pi)} \frac{\int dp \frac{p^3}{m_t} F^*(\mathbf{p}, E) G(\mathbf{p}, E)}{\int dp\, p^2 |G(\mathbf{p}, E)|^2} \quad . \tag{14}$$

The corresponding formulae are given in [8, 12]. The function $\Phi(E)$ was first considered in [13]. Since the approach of [10] has not been extended yet to the case of p–wave, we include Higgs effects only through the effective potential (5) when evaluating the function $\Phi(E)$.

Fig.1(b) shows the real (Φ_{R}) and the imaginary (Φ_{I}) part of the function $\Phi(E)$ for two different values of the Higgs mass in comparison to the case of a pure QCD–potential.

One can see that while the imaginary part grows with decreasing Higgs mass, the real part gets smaller with the effect being stronger for the real part. The dependence of Φ_{I} on M_H below threshold is almost negligible while it gets comparable to that of Φ_{R} for larger energies. For Φ_{R} it amounts about 10–20% over the whole range.

Turning to octet $t\bar{t}$–production, the group factor becomes $C_R = 1/6$. The effective potential is now repulsive, so that below threshold the cross section essentially vanishes with a small smearing caused by the non–zero width of the top quark. Fig.3 shows the threshold factor (13) for the octet case. Again the solid line corresponds to the case of a pure QCD–potential and the dashed one to V_{eff} with $M_H = 100$ GeV.
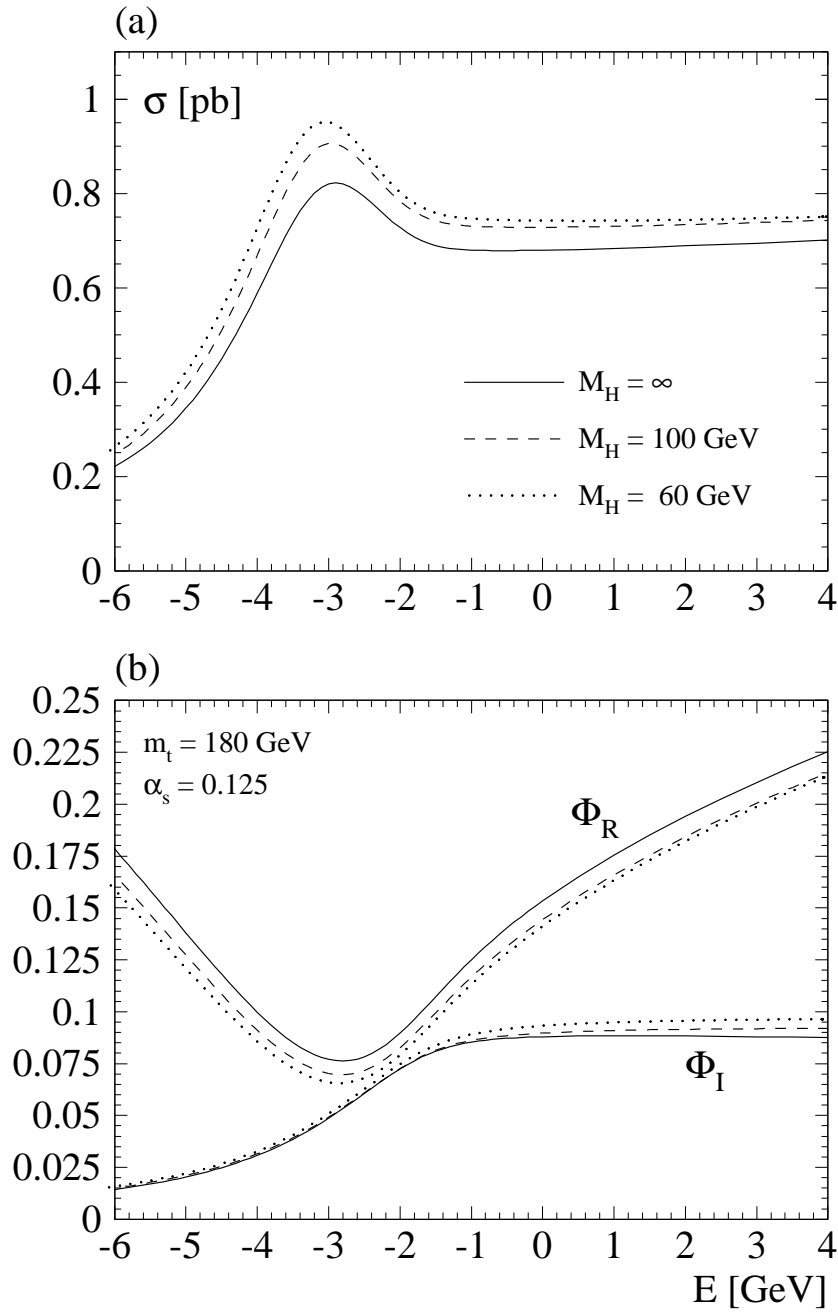
4

Figure 1: Higgs effects in $e^+e^- \to t\bar{t}$ production for (a) the total cross section for unpolarized $e^\pm$ and (b) the real (Φ_R) and imaginary (Φ_I) part of the function $\Phi(E)$ (see eq.(14)) for $M_H = 60$ GeV (dotted), $M_H = 100$ GeV (dashed) and $M_H \to \infty$ (solid).
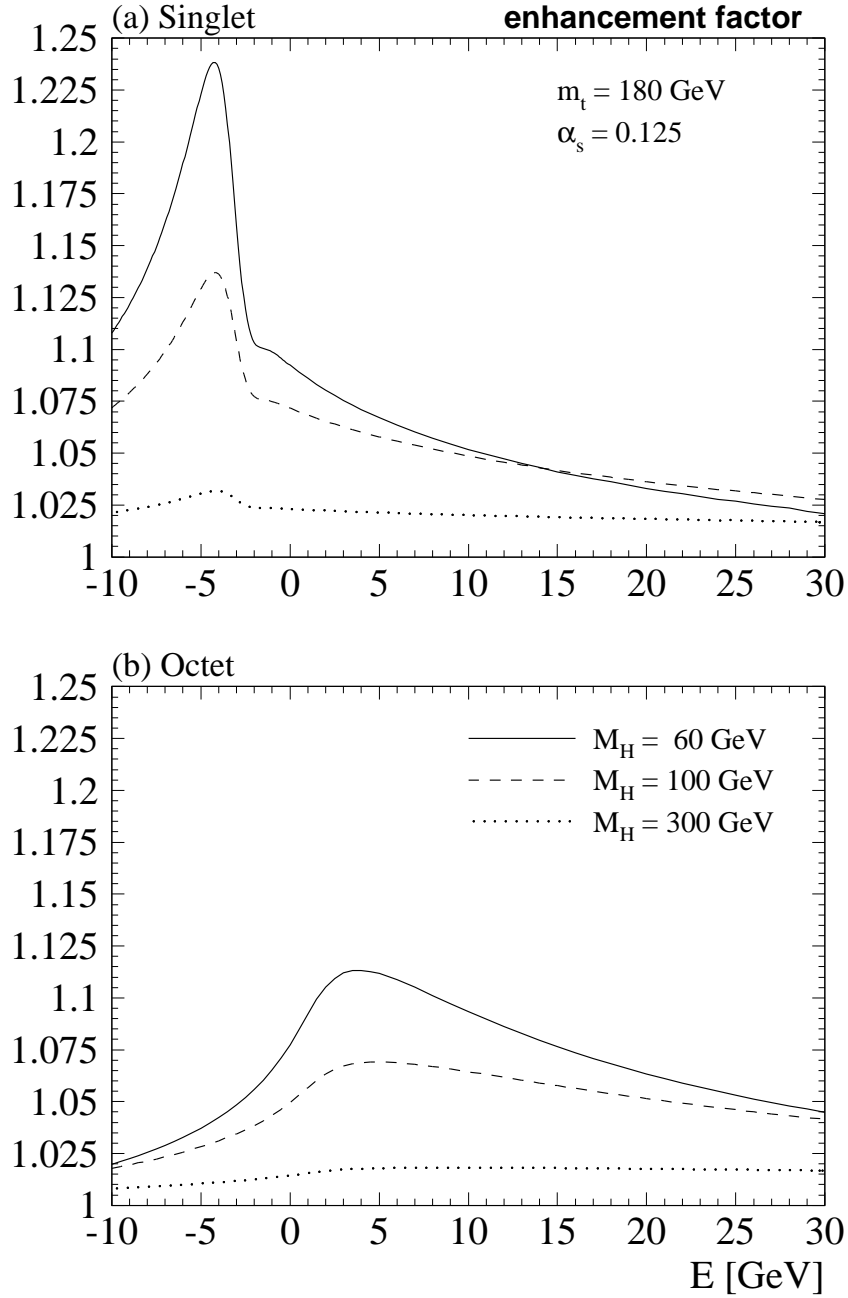
5

Figure 2: Enhancement factors due to exchange of a Higgs boson of mass $M_H = 60$ (solid), 100 (dashed) and 300 GeV (dotted) in $t\bar{t}$–system: (a) singlet and (b) octet color configuration.
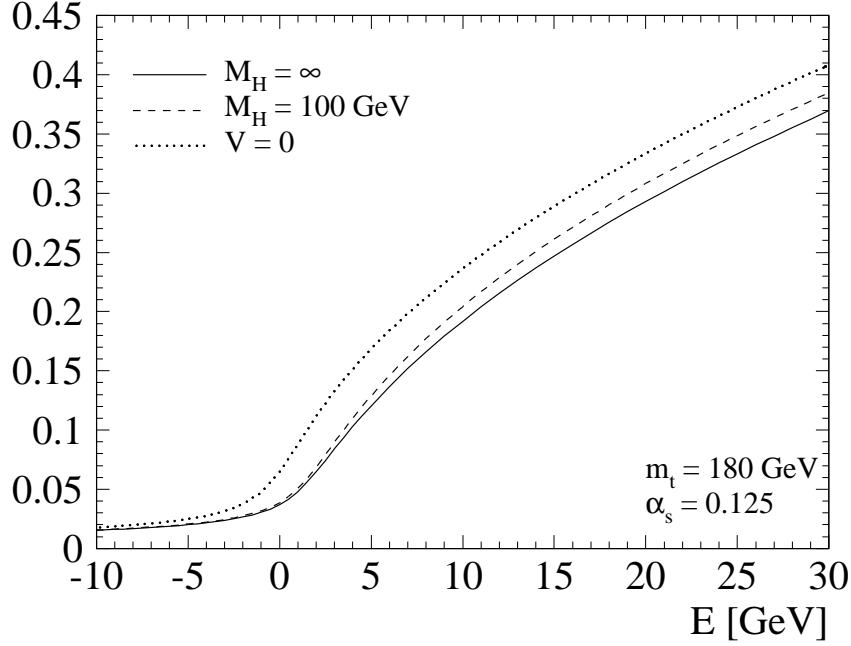
Figure 3: Comparison of phase space factors $B(E)$ (13) for $t\bar{t}$ octet production, including QCD and Higgs effects for $M_H = \infty$ (solid line) and $M_H = 100$ GeV (dashed). The dotted line corresponds to production of free unstable quarks, cf. eq.(15).

The dotted line is now the phase space factor for free unstable particles

$$B^{(free)}(E) = \sqrt{\frac{\sqrt{E^2 + \Gamma_t^2} + E}{2m_t}} \quad , \qquad (15)$$

evaluated by inserting the free Greens function (3) into the right hand side of (13). For the pure QCD–potential the "effective" threshold is shifted towards larger energies compared to the free case and the magnitude is lowered. Higgs exchange cancels these effects to some extent.

As can be seen from fig.2(b), the enhancement factor is smoother than for the singlet case. It is also smaller with a maximum of 11–12% for $M_H = 60$ GeV, going down to less than 2% for $M_H = 300$ GeV, when the shape of the curve becomes almost totally flat.

References

[1] F. Abe *et al.* (CDF Collaboration), *Phys. Rev. Lett.* **74** (1995) 2626.

[2] S. Abachi *et al.* (DØ Collaboration), *Phys. Rev. Lett.* **74** (1995) 2632.

[3] D. Schaile, in *Proc. of Int. Conf. on High Energy Physics*, Glasgow 1994.

[4] V.S. Fadin and V.A. Khoze, *Proceedings of 24th Winter School of the* LNPI, vol.I, p.3, Leningrad 1989.

[5] V. Fadin, V. Khoze and T. Sjöstrand, *Z. Phys.* **C 48** (1990) 613.
    V. Fadin and O. Yakovlev, *Sov. J. Nucl. Phys.* **53** (1991) 1053.

[6] M.J. Strassler and M.E. Peskin, *Phys. Rev.* **D 43** (1991) 1500.

[7] M. Jeżabek, J.H. Kühn and T. Teubner, *Z. Phys.* **C 56** (1992) 653.

[8] R. Harlander, M. Jeżabek, J.H. Kühn and T. Teubner, *Phys. Lett.* **B 346** (1995) 137.

[9] M. Jeżabek and T. Teubner, *Z. Phys.* **C 59** (1993) 669.

[10] M. Jeżabek and J.H. Kühn, *Phys. Lett.* **B 316** (1993) 360.

[11] R.J. Guth and J.H. Kühn, *Nucl. Phys.* **B 368** (1992) 38.

[12] R. Harlander, M. Jeżabek, J.H. Kühn and M. Peter, in preparation.
     M. Jeżabek, *Act. Phys. Pol.* **B 26** (1995) 789.

[13] H. Murayama and Y. Sumino, *Phys. Rev.* **D 47** (1993) 82.